Towards Hybrid Control of a Flexible Curvilinear Surgical Robot With Visual/Haptic Guidance

Liao Wu, Keyu Wu, and Hongliang Ren

***Abstract*— Comprised of multiple telescoptic precurved tubes that can independently rotate and translate, concentric tube robots (CTRs) are favorable in minimally invasive surgeries thanks to their small size and considerable dexterity along with curvilinear accessibility. However, there is a lack of investigation on improvement of the surgeons' perception which in turn can be used to guide the telemanipulation. In this work, we proposed an eye-in-hand configuration for the concentric tube robot by adding an endoscope to the tip of the inner tube, which provides direct and intuitive visual sensing ability for the operator. Based on this visual feedback, we further developed two frameworks for the hybrid control of CTR, namely Teleoperation Before Visual Servoing (TBVS) and Teleoperation During Visual Servoing (TDVS). The structures of these two frameworks were elaborated with key algorithms derived. The effectiveness of the proposed methods were demonstrated through a series of experiments both in free space and in a confined environment (inside a skull model). The results manifested that the visual guidance had the potential of assisting the operator to control the CTR more efficiently.**

I. INTRODUCTION

Continuum robots have emerged as promising instruments in minimally invasive surgeries because of their considerable dexterity and intrinsic safety compared with rigid competitors. In the last decade, concentric tube robots (CTRs), a class of continuum robots consisting of multiple pre-curved telescopic tubes, have found various application scenarios including intracardiac procedures [1], urology surgeries [2], vitrectomy [3], transoral/transnasal procedures [4], [5], [6], [7], orthopedic surgeries [8], et al.

As the principle of this kind of robots is mainly based on the interaction among super-elastic tubes with different pre-curvatures and stiffness, control of the robots usually leverages the technique of teleoperation, in which the operator's input motions are exerted onto a haptic device and mapped to the tip of the CTR through a complicated model [9]. While it significantly enhances surgeons' capability of manipulation in a confined space inside human body through a small open orifice/incision, there remain two issues to be further intensively studied, including

1) how to improve the surgeon's perception of the robot and the environment so that the surgeon can better understand the situation at the surgical site, and
2) how to use the perception to endow the robot certain level of autonomous motion so as to guide the surgeon's manipulation and reduce the surgeon's burden.

There have been some researches addressing the perception of CTRs since they were proposed for minimally invasive surgeries. For example, electromagnetic coil was used to track the orientation and position of the distal tip of CTR [5]. Other sensing methods include fluoroscopy [10], 3D ultrasound [11], [12], X-ray [13], MRI [14], and CT images [15]. While these methods can be feasible and favorable in some specific applications, they have their own limitations as well. For instance, the electromagnetic tracking system is susceptible to the interference from ferromagnetic material within the working area. The tomographic imaging methods mentioned above rely on expensive imaging equipments and detection of CTR in these imaging modalities are very challenging. Besides, these methods are mainly helpful in delivering the robot to some specific locations inside the body, but not competent in displaying the manipulation of the instrument at the surgical sites due to their unintuitive nature. In contrast, direct vision from endoscopes provides intuitive perception of CTR at a relatively cheap cost and generally sets few requirements of the hardware system. Considering this, we propose an eye-in-hand visual guidance configuration for CTR by integrating a micro endoscope to the robot system, as shown in Fig. 1. In this configuration, a robot is constructed by at least two telescopic tubes that are in charge of delivering an instrument inserted through

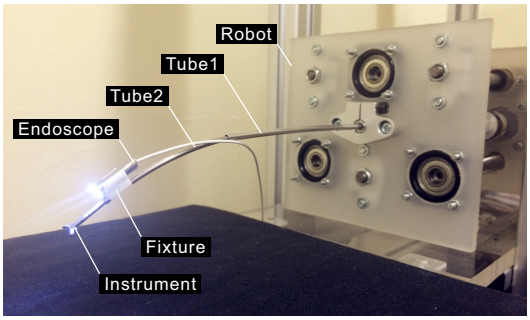

Fig. 1. The proposed eye-in-hand configuration for the CTR, in which a micro endoscope is fixed onto the tip of the inner tube to provide visual feedback.

This work was supported in part by the Singapore Academic Research Fund under Grant R-397-000-227-112 and Singapore Millennium Foundation under Grant R-397-000-201-592 awarded to Dr. Hongliang Ren, and in part by the Vice-Chancellor's Research Fellowship from Queensland University of Technology under Grant 322450-0096/08 awarded to Dr. Liao Wu.

Liao Wu is with the Australian Centre for Robotic Vision, Queensland University of Technology, Brisbane, QLD 4000, Australia. He was a research fellow with the Department of Biomedical Engineering, National University of Singapore, 117575, Singapore wuliaothu@gmail.com/liao.wu@qut.edu.au

Keyu Wu and Hongliang Ren are with the Department of Biomedical Engineering, National University of Singapore, 117575, Singapore keyu_wu@nus.edu.sg, ren@nus.edu.sg

the lumen of the inner tube to the target surgical sites, and a micro endoscope is fixed onto the tip of the inner tube to assist in steering the tubes and observing the instrument during manipulation.

Integration of visual feedback allows the robot to incorporate certain level of autonomous motion by means of visual servoing, a useful technique widely studied for industrial and medical robots [16], [17]. Surprisingly, there has been limited research literature reporting application of this technique to the control of CTR. Ref. [18] investigated the kinematics of CTR with application of position-based visual servoing, which requires calibration of the camera and is sensitive to the kinematic modeling error of the robot. Ref. [19] proposed an eye-to-hand configuration for CTR and developed a model-free image-based visual servoing algorithm. However, this configuration assumes the camera to be observing the tubes from a side viewpoint and thus requires large setup space, leading to difficulty in a practical surgery. In this work, we will tailor this model-free visual servoing algorithm to fit the proposed eye-in-hand configuration, which is much more compact for surgical applications.

Further more, we will investigate how to incorporate this visual feedback into the framework of controlling CTR with the aim of delivering the robot to the desired surgical targets efficiently and accurately. A straightforward way is to concatenate the process of teleoperation and that of visual servoing successively. In this framework, first the surgeon teleoperates the robot to approach the target position, and then the robot automatically searches and moves to the target position through visual servoing (teleoperation before visual servoing, or TBVS). While conventional model-free visual servoing methods [20], [19] require a separate initialization procedure to estimate the image Jacobian matrix, we propose in this work that the image Jacobian matrix can be obtained during the teleoperation process, making the connection between teleoperation and visual servoing seamless and the framework more fluent.

Another way of using this visual feedback is to integrate the visual servoing process into the framework of teleoperation (teleoperation during visual servoing, or TDVS). In general, there have been quite a few established studies on augmentation of teleoperation systems using sensing feedback (a review of these studies can be found in [21]). Ref. [22] investigated the effectiveness of using haptic guidance to steer an endoscope. The technique of virtual fixture [23], which was developed to enhance human-machine interaction for industrial and medical robots, is most related to the task defined in this work. Ref. [24] proposed a method of using virtual fixtures in vision-assisted control of a Steady Hand Robot. However, this robot was manipulated in a cooperative manner rather than by teleoperation, and it was not clear how the visual feedback was mapped with the motion of the robot. In this work, we will investigate the method of using the information generated by the model-free visual servoing algorithm to guide the manipulation of the CTR.

The contributions of this paper are summarized as follows.

1) We propose a method of fluently connecting the teleoperation and model-free visual servoing processes for the CTR with eye-in-hand configuration by performing the estimation of initial image Jacobian matrix at the teleoperation stage;
2) We put forward a framework of integrating the teleoperation and model-free visual servoing processes so that the CTR can be always controlled by the surgeon while guidance from the model-free visual servoing algorithm can be used to enhance the efficiency of manipulation.

The remaining part of this paper is organized as follows. In Section II, we first introduce the model-free visual servoing algorithm, and then elaborate the TBVS and TDVS frameworks for hybrid control of the robot based on visual feedback. Several groups of experiments have been conducted to demonstrate the effectiveness of the proposed methods and are described in Section III. A further discussion of the two frameworks and a conclusion of the paper are drawn in Section IV.

II. METHOD

A. Model-Free Visual Servoing Algorithm

1) Image Processing: In this work, two types of markers are used to indicate the location of the target and the task defined in this project is to steer the CTR so that the instrument inside the lumen of the CTR can reach the target. As the position of the instrument extended out with a certain length can be calibrated on the image of the endoscope, the task can be converted into letting the marker coincide with the calibrated desired position on the image. The patten of the marker is either a yellow square one that is glued at the target, or a light spot produced by a laser projector pointing at the desired site. Note that these markers are used for preliminary validation of the proposed methods; in a practical surgery, the markers can be produced either by the manners demonstrated in this work, or by tracking some special features existing in the environment, depending on the actual task and environment faced.

The images captured by the endoscope are processed by following the procedure shown in Fig. 2. Firstly, the captured image is converted from RGB image to HLS image and the marker is highlighted based on the threshold determined by hue, lightness and saturation. The yellow marker is mainly detected according to the hue value. For the laser marker, however, since the pattern produces a light white area on the image, only light and less saturated pixels are preserved. However, due to the limited resolution and sharpness of the micro-camera, the extracted target contains discontinuous pixels and therefore requires to be further processed. To this end, dilation and erosion is implemented to repair the extracted target and ensure its integrity. Subsequently, canny edge detection is adopted to find the contour of the target. The idea is to use a Sobel kernel in both horizontal and vertical directions by applying a pair of convolution masks so that the intensity gradient G together with intensity direction θ can be figured out for each pixel.

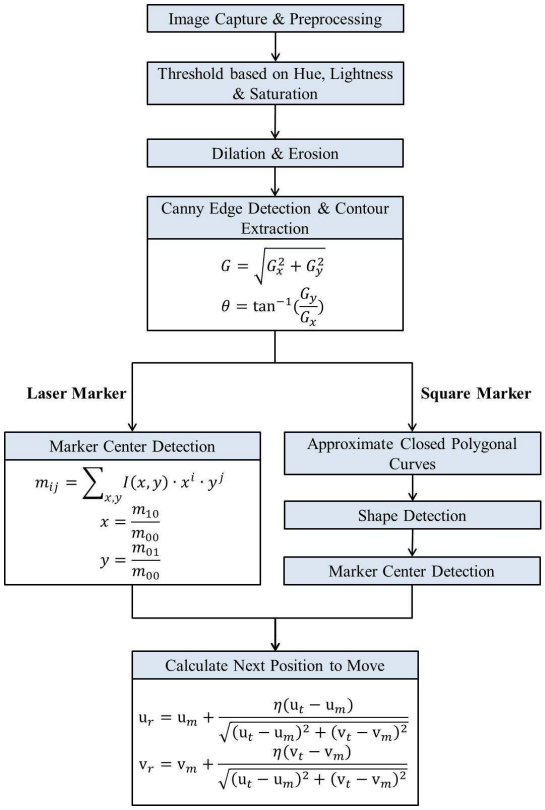

Fig. 2. The image processing algorithm.

For the laser marker, the resultant pixels are accepted as an edge if its gradient is higher than the threshold or connected to a pixel that is above the threshold, which is set as 150 empirically. The moment of the contour is introduced to calculate the location of the target (as shown in Fig. 2, m_{ij} represents the raw image moments [25], and x and y stand for the center of the target).

For the yellow square marker, the square shape is detected by approximating the contours to closed polygonal curves and the center of the marker is indicated by the center of the square.

Detecting the current location of the marker, the algorithm automatically calculates the next desired position on the image for the marker to reach, i.e., (u_r, v_r). It is defined as η units away from the current position in the direction radiated from current position (u_m, v_m) to the goal position (u_t, v_t). However, when the distance between current position and the goal position is less than η, the next position to reach is directly the goal position. Once the distance between the target and the goal position is less than ε pixels (in this paper ε is set as 5), the target is regarded as reaching the desired location.

2) Model-Free Visual Servoing: Usually, the model-free visual servoing requires an initialization procedure to acquire the initial image Jacobian matrix, which is defined as

$$J_0 = \begin{bmatrix} \frac{\partial f(q)}{\partial q_1} & \frac{\partial f(q)}{\partial q_2} & \cdots & \frac{\partial f(q)}{\partial q_n} \end{bmatrix} \quad (1)$$

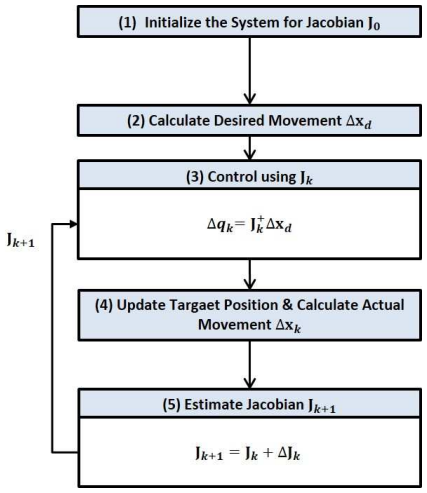

Fig. 3. The model-free control algorithm. Joint motion is calculated by using the estimated Jacobian while the Jacobian matrix is iteratively updated based on the visual feedback.

where $f(q)$ is the target position in the image coordinate system while q_i is the i-th joint input, and n is the number of involved joints. It is obtained by running each joint of the robot separately and measuring the position change of the marker in the image space.

Generally, the control algorithm includes two key steps, one to calculate the required joint motion using an estimated Jacobian matrix and the other to update the Jacobian matrix based on visual feedback, as shown in Fig. 3.

Joint motion Δq_k is calculated by following equation (2) where $J_k^{\dagger}$ is the psudo-inverse of the estimated Jacobian J_k at time k, and Δx_d represents the desired movement of the robot at time k, that is, the coordinate difference between the current position and the next position to reach. The simple minimum norm solution is utilized here.

$$\Delta q_k = J_k^{\dagger} \Delta x_d \quad (2)$$

As the robot moves, the Jacobian matrix has to be updated constantly not only because the Jacobian is generally not estimated precisely but also due to the continuous change in Jacobian in constrained environments. Therefore the actual movement of the marker on the image plane is measured and used as feedback to constantly update the estimated Jacobian matrix. Under the assumption that the Jacobian matrix varies little after each movement of the robot, the objective of the Jacobian estimation step can be formulated as

$$min \ ||\Delta J_k||_F \quad s.t. \quad \Delta x_k = (J_k + \Delta J_k)\Delta q_k \quad (3)$$

where Δx_k is the actual movement of the marker in the image coordinate system and Δq_k is the actuated movement of each joint. Using Broyden's updating method [26], the minimum norm solution to this problem can be found by

$$\Delta J_k = (\Delta x_k - J_k \Delta q_k)(\Delta q_k^T \Delta q_k)^{-1} \Delta q_k^T. \quad (4)$$

Then the updated Jacobian J_{k+1} can be estimated as

$$J_{k+1} = J_k + \alpha \Delta J_k \tag{5}$$

where α is a damping factor and is set as 0.1 in this paper.

By iteratively implementing the optimal control algorithm and the Jacobian estimation algorithm, the robot can be controlled to ensure that the target is moved to the desired position on the image plane and subsequently kept at that position despite the movements caused by external disturbance.

B. Teleoperation Before Visual Servoing (TBVS)

A hybrid control strategy can be constructed by an alternation between teleoperation and visual servoing. Teleoperation, leveraging the operator's visual and/or haptic sensing and intelligence, is intuitive and flexible, and outperforms in obstacle avoidance. Visual servoing, on the other hand, provides active and accurate tracking ability, which is desirable for targeting non-stationary objects and resisting unexpected perturbation. Therefore, it is beneficial to combine the complementary advantages of both methods. A possible way, for example, is to first tele-operate the robot to approach the target, and then start the visual servoing process so that the target can be real-time tracked.

It is noted that when this strategy is adopted, the initial Jacobian matrix for the model-free visual servoing can be estimated from the teleoperation process. Suppose at time k, the robot is to be changed from teleoperation to visual servoing. Then, m past states of (x,q) are sampled and recorded, where x is the position of the target point in the image space and q is the joint position (see Fig. 4). By subtracting these states variables by the state at time k, m incremental variables are obtained. We have

$$\Delta x_k^1 = J_0 \Delta q_k^1 \tag{6}$$
$$\Delta x_k^2 = J_0 \Delta q_k^2 \tag{7}$$
$$\cdots$$
$$\Delta x_k^m = J_0 \Delta q_k^m \tag{8}$$

and, by combining (6)-(8), we can obtain,

$$\Delta X_k = J_0 \Delta Q_k. \tag{9}$$

Since a more distant state provides less accurate information, a weight matrix $W_k = diag(||\Delta q_k^1||, ||\Delta q_k^2||, \cdots, ||\Delta q_k^m||)^{-1}$ might be used to normalize each column of ΔQ_k, and thus we have

$$\Delta X_k W_k = J_0 \Delta Q_k W_k. \tag{10}$$

The least square solution is given by

$$J_0 = \Delta X_k W_k (\Delta Q_k W_k)^T (\Delta Q_k W_k W_k^T \Delta Q_k^T)^{-1}. \tag{11}$$

A limitation of this approach is the possibility of obtaining an ill conditioned Jacobian matrix when the teleoperation trajectory before the switch point is degenerate, i.e., does not include contributions of every actuator. Therefore, the condition number of the Jacobian matrix will be examined and if it is ill conditioned, more samples are collected to increase the condition number.

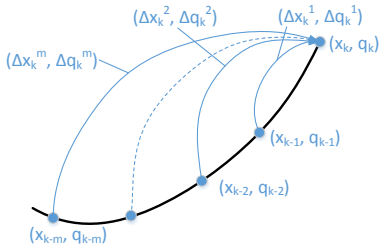

Fig. 4. Guessing an initial Jacobian matrix from teleoperation trajectory.

C. Teleoperation During Visual Servoing (TDVS)

Another framework for hybrid control of CTR is to integrate the advantages of teleoperation and visual servoing simultaneously, as shown in Fig. 5. Considering the superiority of human in dealing with unexpected disturbance efficiently and dexterously, this framework sets teleoperation of human as the most direct control of CTR. At the same time, the visual feedback provided by the endoscope attached to the tube is also utilized by generating a guiding force which is rendered to the haptic device.

From Fig. 5 we can see that the robot motion is controlled by the mapping of the master position (the input of the haptic device), which is determined jointly by the operator's manipulation and the guiding force generated by the visual servoing algorithm. The basic structure of the visual servoing algorithm is similar to the one described in Section II-A. The main difference lies in that the algorithm does not generate command to drive the motors to the desired position directly, but produces a guiding force and renders it onto the haptic input device. As a result, the operator feels a guiding force pulling the input stylus to the desired position while teleoperating the robot. However, the operator is still able to disobey this guidance and adjust the real input by exerting his own force onto the stylus, which is favorable in a surgical environment since human is generally more reliable than visual servoing algorithms.

Since the basic model for visual servoing have been established in previous sections, the remaining key point is how to render the guiding force onto the input device. As introduced in Section II-A, the visual servoing algorithm automatically derives the desired motor positions at the end of each iteration step. Using these motor positions, we are able to calculate the desired master position thanks to the forward kinematics of the robot and the spatial mapping between the master and the slave. Now suppose the calculated desired master position is denoted as P_d, and the actual master position that is sampled from the controller of the device is denoted as $P_a(t)$ (the actual position is variable upon sampling time t). We use a spring model to describe the behavior of the guidance, i.e.,

$$F = \begin{cases} \beta(P_d - P_a(t)) & : \quad 0 < ||P_d - P_a(t)|| < \frac{F_{max}}{\beta} \\ F_{max} & : \quad ||P_d - P_a(t)|| \geq \frac{F_{max}}{\beta} \end{cases} \tag{12}$$

where β is the stiffness of the spring, and F_{max} is the maximum force allowed. In this work, β and F_{max} are set

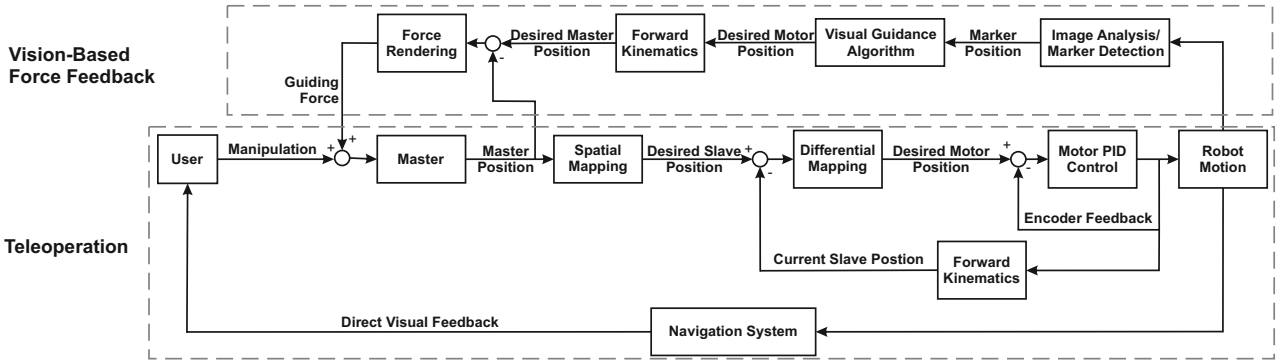

Fig. 5. The proposed framework for Teleoperation During Visual Servoing.

as 1 N/mm and 1 N, respectively.

In addition, in order to stabilize the transition from the state of no force to the state of with force, we need to add a smoothing function to avoid a sudden exerted onto the operator. Simply but effectively, we multiply the force with a linear function of time t, where t restarts from zero every time the anchor position changes. The force is calculated as below,

$$f = \gamma(t)F \tag{13}$$

where

$$\gamma(t) = \begin{cases} \frac{t}{T} & : \quad 0 \leq t < T \\ 1 & : \quad t \geq T \end{cases} \tag{14}$$

where T is empirically set as 100 ms in the experiments.

III. EXPERIMENTS

A. Experiment I: TBVS

1) Free Space: In this group of experiments, we will test the TBVS method in free space using the setup shown in Fig. 6. The robot consisted of a curved inner tube and a straight outer tube. A micro camera was attached to the tip of the inner tube to provide visual feedback. At the beginning, the square marker was not in sight and the teleoperation was implemented to guide the movement of robot until the marker was within the visual field. When the marker appeared in the image captured by the camera, the locations of the marker were measured while changing the joint positions using the Geomagic Touch. The initial Jacobian was then determined using the method introduced in the hybrid control section. After initialization, the teleoperation control mode was replaced by the visual servoing control mode to move the marker to and maintain the marker at the target location in the visual field.

To investigate the impacts of the number of used incremental variables on the accuracy of the visual servoing control algorithm, different numbers of incremental variables were used for initialization and the differences between the reference and actual trajectories were noted down for different step lengths. For each step length, the experiment was repeated for four times. The mean differences between the reference and actual trajectories as well as the standard deviations are depicted in Fig. 7. We can see that the accuracy

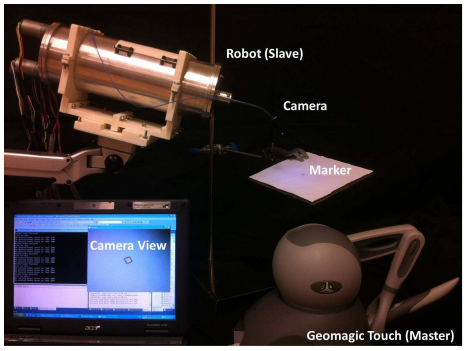

Fig. 6. Experiment setup in free space. A yellow square marker is used as target.

of the algorithm improves with reduced step length. However, the number of incremental variables used for Jacobian initialization has little effect on the performance of the visual servoing. The reason for this is inferred as follows. Although theoretically more samples of the incremental variables should minimize the impact of noise to the estimation of the initial Jacobian matrix, it also introduces more inaccurate information as the distance of the incremental variable gets larger. The final effect is a compromise. As a result, the relationship between the number of incremental variables used and the quality of the successive visual servoing process cannot be quantitatively determined.

2) Skull Model: Another experiment on TBVS was conducted inside a skull model. Instead of a square marker, a laser pointer was used to create a red dot at the target position inside the skull model as shown in Fig. 8. Similarly, at the beginning, the laser marker was not in sight and the teleoperation was implemented to guide robot to pass through the nasal cavity until the marker appeared in sight (see Fig. 9). The initial Jacobian matrix was then calculated by measuring the locations of the marker on the image plane when changing the joint positions using the Geomagic Touch for several times. After initialization, the teleoperation control mode was switched to the visual servoing control mode to move the marker to and maintain the marker at the target location in the visual field.

Besides, a needle was inserted inside the robot in advance

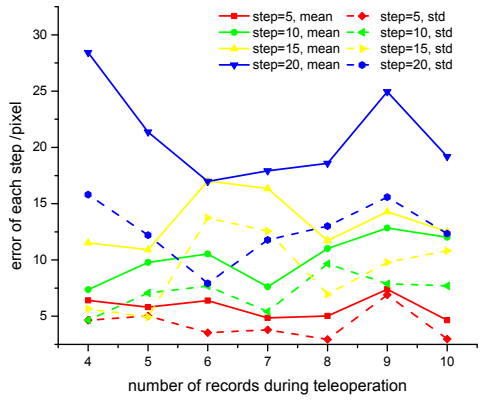

Fig. 7. Error between the reference trajectories and the actual trajectories in hybrid control of the CTR in free space.

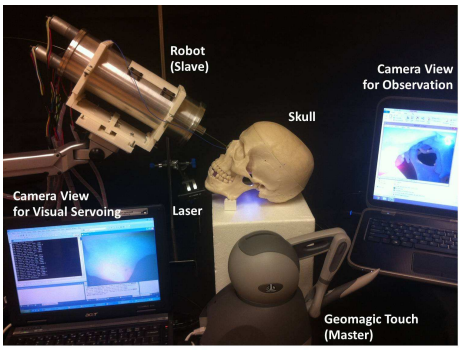

Fig. 8. Experiment setup inside a skull model. The laser pattern is used as target.

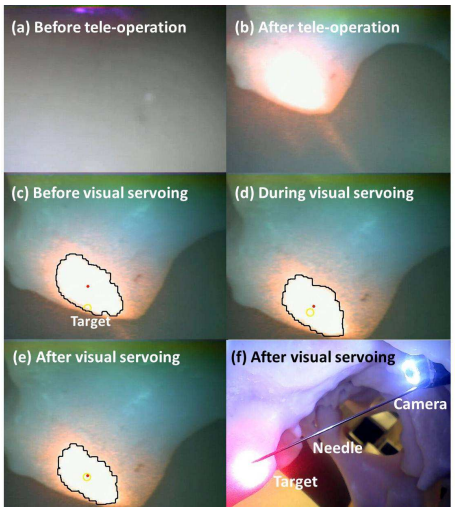

Fig. 9. Experiment implemented inside the skull model. (a) Before teleoperation, (b) After teleoperation, (c) Before visual servoing, (d) During visual servoing, (e) After visual servoing, (f) Needle insertion after visual servoing.

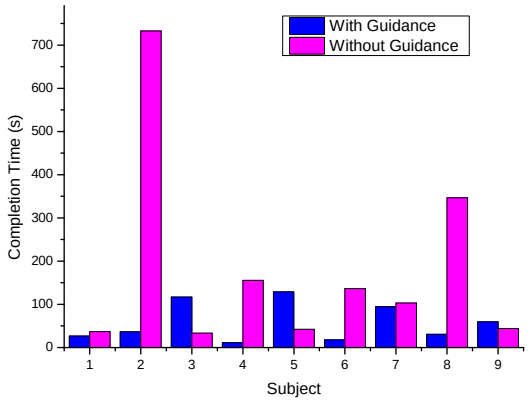

Fig. 10. Comparison of the completion time between with guidance and without guidance on nine subjects.

and used to better visualize the efficiency of the proposed hybrid control algorithm. As indicated in Fig. 9, after the experiment, the needle was extended outside the robot and successfully touched the target position, which articulates the feasibility and accuracy of the proposed hybrid control approach. It can then be concluded that the proposed control algorithm is able to bring the surgical tools to desired locations precisely in a confined environment.

B. Experiment II: TDVS

To validate the second framework for the hybrid control of the CTR, i.e., the TDVS method, we carried out another group of experiments using a similar setup as shown in Fig. 6 except that the robot was replaced by the one appearing in Fig. 1 and the marker was replaced by a laser point. In this experiment, nine subjects were invited to steer the robot so that the marker was moved to the desired position on the image. Each subject was asked to perform two groups of contrast experiments. In the first group, the subject completed the task with guiding force adding to the input haptic device. That is, the subject first teleoperated the robot to approach the marker, and then started fine manipulation with a guiding force rendered. The way of generating the guiding force has been described in Section II-C. In the second group, the subject completed the task on his/her own without any force exerted from the haptic device. In order to make a fair contrast, the starting points of both groups of experiments are approximately the same.

The completion time, meaning the time from the very beginning to the moment of reaching the target, was recored and shown in Fig. 10. It can be seen that in six of nine cases (66.7%), the subject performed faster with a guiding force than without guidance. It is also observed that the situation where no guidance is incorporated correlates to a higher possibility of abnormal length of completion time. This is mainly because it is difficult for the subject to do the fine adjustment of the motion of the CTR when it is near the target position. The results indicate the advantages of the proposed hybrid control method with visual guidance.

IV. DISCUSSION AND CONCLUSION

In this paper, we have proposed an eye-in-hand configuration for the concentric tube robot by attaching an endoscope to the tip of the inner tube. Based on this visual feedback,

we further developed two frameworks for hybrid control of CTR, namely TBVS and TDVS. The effectiveness of the proposed methods have been demonstrated through a series of experiments both in free space and in a confined environment (inside a skull model). The results showed that the visual guidance had the potential of assisting the operator to control the CTR more efficiently.

We would like to emphasize that although some preliminary results have been achieved in this paper, there are still much work to do to improve the frameworks. For the TBVS, methods to inspect and avoid occurrence of singularity during teleoperation are needed, as the visual servoing algorithm is sensitive to the quality of the initial estimation of the image Jacobian matrix. In addition, it is also interesting to investigate how to enhance the safety guaranty when letting the robot automatically reach the target.

For the TDVS, extra efforts should be paid to the force rendering manner. In this work we have used a simple spring model to generate the guiding force. However, there are many other candidates and we need to figure out which provides the best haptic experience in guiding the operator to the desired position. The role adaption issue emerging in the shared control of the robot is also very important and needs further study.

Finally, as TBVS involves a part of autonomous control by the robot itself, the framework has more potential in reducing the surgeon's burden but raises the concern of safety. On the other hand, the TDVS framework always gives the control handle to the surgeon which is more robust. However, the guidance may violate the intention of the surgeon due to imperfection of the visual sensing quality and thus cause undesired consumption of efforts. Therefore, a more comprehensive comparison between these two frameworks are very useful and will be conducted in our future work.

REFERENCES

[1] A. H. Gosline, N. V. Vasilyev, E. J. Butler, C. Folk, A. Cohen, R. Chen, N. Lang, P. J. del Nido, and P. E. Dupont, "Percutaneous intracardiac beating-heart surgery using metal mems tissue approximation tools," *The International Journal of Robotics Research*, vol. 31, no. 9, pp. 1081–1093, 2012.

[2] R. J. Hendrick, S. D. Herrell, and R. J. Webster, "A multi-arm hand-held robotic system for transurethral laser prostate surgery," in *2014 IEEE International Conference on Robotics and Automation (ICRA)*, pp. 2850–2855, 2014.

[3] L. Wu, B. L.-W. Tan, and H. Ren, "Prototype development of a hand-held robotic light pipe for intraocular procedures," in *2015 IEEE International Conference on Robotics and Biomimetics (ROBIO)*, pp. 368–373, 2015.

[4] K. Wu, L. Wu, C. M. Lim, and H. Ren, "Model-free image guidance for intelligent tubular robots with pre-clinical feasibility study: Towards minimally invasive trans-orifice surgery," in *2015 IEEE International Conference on Information and Automation (ICIA)*, pp. 749–754, 2015.

[5] J. Burgner, D. C. Rucker, H. B. Gilbert, P. J. Swaney, P. T. Russell, K. D. Weaver, and R. J. Webster, "A telerobotic system for transnasal surgery," *IEEE/ASME Transactions on Mechatronics*, vol. 3, no. 19, pp. 996–1006.

[6] H. Yu, L. Wu, K. Wu, and H. Ren, "Development of a multi-channel concentric tube robotic system with active vision for transnasal nasopharyngeal carcinoma procedures," *IEEE Robotics and Automation Letters*, vol. 1, no. 2, pp. 1172–1178, 2016.

[7] L. Wu, S. Song, K. Wu, C. M. Lim, and H. Ren, "Development of a compact continuum tubular robotic system for nasopharyngeal biopsy," *Medical and Biological Engineering and Computing, in press*, 2016.

[8] K. Wu, L. Wu, and H. Ren, "Motion planning of continuum tubular robots based on centerlines extracted from statistical atlas," in *2015 IEEE/RSJ International Conference on Intelligent Robots and Systems (IROS)*, pp. 5512–5517, 2015.

[9] P. E. Dupont, J. Lock, B. Itkowitz, and E. Butler, "Design and control of concentric-tube robots," *IEEE Transactions on Robotics*, vol. 26, no. 2, pp. 209–225, 2010.

[10] J. Burgner, S. D. Herrell, and R. J. Webster, "Toward fluoroscopic shape reconstruction for control of steerable medical devices," in *ASME 2011 Dynamic Systems and Control Conference and Bath/ASME Symposium on Fluid Power and Motion Control*, pp. 791–794, 2011.

[11] H. Ren and P. E. Dupont, "Tubular structure enhancement for surgical instrument detection in 3D ultrasound," in *2011 Annual International Conference of the IEEE Engineering in Medicine and Biology Society*, pp. 7203–7206, 2011.

[12] H. Ren and P. E. Dupont, "Tubular enhanced geodesic active contours for continuum robot detection using 3D ultrasound," in *2012 IEEE International Conference on Robotics and Automation (ICRA)*, pp. 2907–2912, 2012.

[13] E. J. Lobaton, J. Fu, L. G. Torres, and R. Alterovitz, "Continuous shape estimation of continuum robots using X-ray images," in *2013 IEEE International Conference on Robotics and Automation (ICRA)*, pp. 725–732, 2013.

[14] H. Su, D. C. Cardona, W. Shang, A. Camilo, G. A. Cole, D. C. Rucker, R. J. Webster, and G. S. Fischer, "A MRI-guided concentric tube continuum robot with piezoelectric actuation: a feasibility study," in *2012 IEEE International Conference on Robotics and Automation (ICRA)*, pp. 1939–1945, 2012.

[15] R. A. Lathrop, D. C. Rucker, and R. Webster, "Guidance of a steerable cannula robot in soft tissue using preoperative imaging and conoscopic surface contour sensing," in *Robotics and Automation (ICRA), 2010 IEEE International Conference on*, pp. 5601–5606, IEEE, 2010.

[16] S. Hutchinson, G. D. Hager, and P. I. Corke, "A tutorial on visual servo control," *IEEE Transactions on Robotics and Automation*, vol. 12, no. 5, pp. 651–670, 1996.

[17] M. Azizian, M. Khoshnam, N. Najmaei, and R. V. Patel, "Visual servoing in medical robotics: a survey. Part I: endoscopic and direct vision imaging–techniques and applications," *The International Journal of Medical Robotics and Computer Assisted Surgery*, vol. 10, no. 3, pp. 263–274, 2014.

[18] R. J. Webster III, J. P. Swensen, J. M. Romano, and N. J. Cowan, "Closed-form differential kinematics for concentric-tube continuum robots with application to visual servoing," in *Experimental Robotics*, pp. 485–494, 2009.

[19] K. Wu, L. Wu, and H. Ren, "An image based targeting method to guide a tentacle-like curvilinear concentric tube robot," in *2014 IEEE International Conference on Robotics and Biomimetics (ROBIO)*, pp. 386–391, 2014.

[20] M. C. Yip and D. B. Camarillo, "Model-less feedback control of continuum manipulators in constrained environments," *IEEE Transactions on Robotics*, vol. 4, no. 30, pp. 880–889, 2014.

[21] C. Passenberg, A. Peer, and M. Buss, "A survey of environment-, operator-, and task-adapted controllers for teleoperation systems," *Mechatronics*, vol. 20, no. 7, pp. 787–801, 2010.

[22] R. Reilink, S. Stramigioli, A. M. Kappers, and S. Misra, "Evaluation of flexible endoscope steering using haptic guidance," *The International Journal of Medical Robotics and Computer Assisted Surgery*, vol. 7, no. 2, pp. 178–186, 2011.

[23] J. J. Abbott, P. Marayong, and A. M. Okamura, "Haptic virtual fixtures for robot-assisted manipulation," in *Robotics Research*, pp. 49–64, Springer, 2007.

[24] A. Bettini, P. Marayong, S. Lang, A. M. Okamura, and G. D. Hager, "Vision-assisted control for manipulation using virtual fixtures," *IEEE Transactions on Robotics*, vol. 20, no. 6, pp. 953–966, 2004.

[25] B. Bamieh and R. De Figueiredo, "A general moment-invariants/attributed-graph method for three-dimensional object recognition from a single image," *IEEE Journal of Robotics and Automation*, vol. 2, no. 1, pp. 31–41, 1986.

[26] C. G. Broyden, "A class of methods for solving nonlinear simultaneous equations," *Mathematics of computation*, vol. 19, no. 92, pp. 577–593, 1965.